Quantitative Damage Criteria of Severely-Damaged Masonry Buildings during the 2008 Wenchuan Earthquake Extracted from Microtremor Records

X. Wang
Disaster Prevention Research Center, Aichi Institute of Technology, Japan

K. Masaki
Department of Urban Environment, Aichi Institute of Technology, Japan

K. Irikura
Disaster Prevention Research Center, Aichi Institute of Technology, Japan

S. Kurahashi
Disaster Prevention Research Center, Aichi Institute of Technology, Japan

SUMMARY:
Masonry buildings are widely used and were severely damaged in the attacked area of the 2008 Wenchuan earthquake. The damage regions during this earthquake are earthquake-prone area in China. In order to prevent this kind of damage from happening in future earthquakes, the damage criteria of masonry buildings should be made clear and provide reference for anti-seismic design and seismic reinforcing of buildings of this structure types. In this study, the damage criteria of buildings with damage level of "severely damaged", which is critical limit for continuous use or demolishment of buildings, are studied based on the changes of time-domain (shear-wave velocities traveling within inner stories) and frequency-domain building response parameters (response frequencies of the ground-foundation-structure system, the upper structure and the soil-structure interaction) extracted from microtremor records measured in severely damaged masonry buildings.

Keywords: Damaged masonry building, Microtremor measurement, Shear-wave velocity, Response frequency

1. INTRODUCTION

Masonry buildings, which are widely used for residential buildings, hospitals, and schools in the source fault zone of the 2008 Wenchuan earthquake, were heavily damaged during this earthquake. Not only in the seismic zone of the 2008 Wenchuan earthquake, but also in other earthquake-prone areas in China, such as the seismic zones of the Yunnan Province, the Qinghai Province and so on, masonry buildings are also widely used and were damaged in previous earthquakes, such as the 2011 M5.8 Yingjiang, Yunnan earthquake and the 2010 Ms7.1 Yushu, Qinghai earthquake. Therefore, reliable damage-level estimation standards of seismic damaged masonry buildings in future earthquakes should be taken into account. Traditionally, building damage levels are determined based on visual check. Though visual check is fast to determine damage levels, it is difficult to reveal the real building damage conditions when invisible damages exist in structural elements. Therefore, in order to evaluate building damage levels more reliably, quantitative building damage criteria corresponding to different damage levels are indispensable. During the 2008 Wenchuan earthquake, damage indexes of 6- and 7-story masonry buildings were the highest compared with masonry buildings with other story numbers (Zhang and Jin, 2008). Besides, based on the on-site building damage investigation performed by our study group, 6-story masonry buildings are very common in the damaged area of this earthquake. It is reasonable to consider 6-story masonry buildings as typical damaged-buildings during the 2008 Wenchuan earthquake. In this paper, quantitative damage criteria of 6-story masonry buildings with damage level of "severely damaged", which is the critical level for judging whether a damaged building can be reinforced or have to be demolished, are proposed based on the changing of shear-wave velocity traveling within stories and response frequencies extracted from microtremor records measured in severely damaged 6-story masonry buildings.

Generally, the response of a building system which is composed of the supporting ground, foundation, and the upper structure can be considered as the summation of responses of the upper structure, and those due to the rigid-body rocking and sway vibration. Corresponding to all these responses, there are four kinds of response frequencies, these are the response frequency of the building system (f_{SYS}), upper structure (f_B), rigid-body rocking (f_R), and the rigid-body sway (f_S). To diagnose the damage of different components of the building system, these response frequencies should be unraveled.

The predominant frequency of the transfer function (the spectral ratio of Fourier spectra of waveforms of the top to that of the base of the building), which is also called apparent frequency f_{app} (Todorovska, 2009), correlates with f_B and f_R as $1/f_{app}^2 = 1/f_B^2 + 1/f_R^2$. When the f_R is big enough, the apparent frequency f_{app} is approximately the same with the f_B, and can be used instead of f_B. However, if the effect of f_R should not be ignored, the f_{app} cannot be used erroneously as f_B. In order to determine the f_B eliminating the effect of ground coupling, the shear-wave velocity propagating in the upper structures, which only depends on structural dynamic properties (shear rigidity), is a reliable means. To extract shear-wave velocity traveling in upper structures, deconvolution with the waveform of the top of a building (in this paper, it is referred as the Deconvolution method for short) which was propose by Snieder and Şafak in 2006 is used in this paper. The physical meaning and an application of this method to earthquake records measured in the Millikan Library in Pasadena, California have been presented by the proposers. In this paper, the feasibility of applying the Deconvolution method to microtremor records is approved based on the comparisons between the shear-wave travel times extracted from microtremor records with those extracted from earthquake records and with theoretical results calculated based on the multi-freedom-degree-system SR mode. To separate the four response frequencies f_{SYS}, f_B, f_R, and f_S, in this paper, after the feasibility of using the Deconvolution method to extract f_B from microtremor records has been proved, an approach to extract the four response frequencies in turn through four steps from the microtremor records measured on the base and the top of the building is proposed as (1) the system frequency f_{SYS} is determined based on the predominant frequency of the power spectra of the microtremor records measured on the top of the building; (2) the response frequency of the upper structure f_B is calculated based on the shear-wave traveling time from the base to the top; (3) the apparent frequency f_{app} is determined from the predominant frequency of the transfer function; (4) the rigid-body rocking and sway frequencies are calculated based on the relationships between these four response frequencies proposed by Luco in 1987 based on vibration tests.

The shear-wave velocities and response frequencies of three 6-story severely damaged masonry buildings are extracted form microtremor records measured in them and are compared with those extracted from a sound 6-story masonry building to evaluate the changes of these parameters which are the damage criteria of the damage level of "severely damaged".

2. DAMAGED BUILDINGS

Microtremor records of three severely damaged masonry buildings locating in the Hanwang town which is reserved as an earthquake relic of the 2008 Wenchuan earthquake were measured. The locations of these three buildings are closed with a red open circle in the Figure 1. Though it is better to obtain the quantitative building damage criteria through comparing response parameters pre- and post-earthquakes, just as what has been done in some previous studies such as the Ohba and Fukuda (1999), Tsurumura and Kawase (2008), Sato et al. (2008), damaged buildings whose microtremors have been recorded before this earthquake are hardly any. In order to get the comparative standard of response parameters, a sound 6-story masonry building locating in the Mianzhu city with good health condition is measured.

Figure 1. Satellite image of the Hanwang town. Locations of the three measured damaged-buildings are marked with the red open circle

Views of the sound building (Building A for short) used as the comparative standard in this paper are shown in the Photo 1. Three sets of observation systems which are consisted of a three-component seismometer, a recorder and a GPS clock are used to measure microtremors. Two of them are fixed on the top floor and the base (the ground floor), respectively. The other was moved from the second floor (2F) to the fifth floor (5F) alternatively each 2 hours. The measure method is generally shown in the Figure 2. Simultaneous microtremors of the top and the inner floors are recorded with the sampling rate f_{samp} of 200 Hz.

The views of a severely-damaged building (Building B for short) are shown in the Photo 2. Obvious X-shaped cracks in the exposed walls of this building because of shearing failure can be seen. Microtremors of all the floors of the Building B were measured in the same way with that performed in the Building A.

Views of another measured severely-damaged building (Building C for short) are shown in the Photo 3. X-shaped cracks in the exposed walls of the 2F can be seen clearly from the Photo 3(a) and the Photo 3(b). Bricks fallen apart from the inner walls of the 2F can be seen from the Photo 3(c) and the Photo 3(d). The measurements were carried out in the same way as shown in the Figure 2.

Views of the Building D, which can also be adjudged as a severely damaged building based on the visible damage check, are shown in the Photo 4. X-shaped cracks in the exposed walls of this building can also be seen. Bricks fallen apart from the inner walls of the ground floor (1F) can be seen in the Photo 4(c) and the Photo 4(d). Not all of the microtremors of the inner floors, but those of the 6F and the 1F are measured in this building.

(a) (b)

Photo 1. The (a) south facade and (b) east facade of the sound 6-floor masonry building (the Building A)

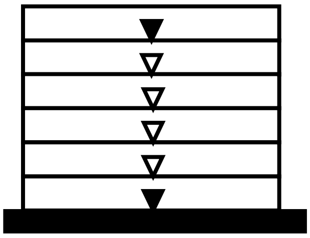

Figure 2. Microtremor measurement of the Building A. The floors measured with fixed observation system are marked with ▼, the floors measured with moving observation system are marked with ▽

(a) (b) (c) (d)

Photo 2. Views of the severely damaged Building B. X-shaped cracks in the exposed wall can be seen

(a) (b) (c) (d)

Photo 3. Views of the severely damaged Building C. X-shaped cracks in the exposed wall can be seen from (a) and (b). Bricks dropped off the inner walls of the 2F can be seen from the (c) and (d)

(a) (b) (c) (d)

Photo 4. Views of the severely damaged Building D. X-shaped cracks in the exposed wall can be seen from (a) and (b). Bricks dropped off the inner walls of the 1F can be seen from the (c) and (d)

3. EXTRACTING SHEAR-WAVE VELOCITY FROM MICROTREMOR RECORDS

3.1 Deconvolution with Waveforms of the Top of Buildings

The Deconvolution method was proposed by Snieder and Şafak (2006) based on the interferometry method which is used to detect the characteristics of geological layers by imaging the floors of the buildings as the geological layers. The basic equation of the Deconvolution method is shown in the equation (3.1).

$$D_{k,Top}(z,\omega) = \frac{u_k(z,\omega)}{u_{Top}(H,\omega)}, \qquad (3.1)$$

Where, $D_{k,Top}(z,\omega)$ is the deconvolved wave (expressed in the frequency domain) with the waveforms of the top, $u_k(z,\omega)$ is the Fourier transform of the horizontal record of the k floor with the representative height of z, $u_{Top}(H,\omega)$ is the Fourier transform of the horizontal response record on the Top with representative height of H. Theoretically, the horizontal response of a floor with the representative height of z can be expressed as equation (3.2).

$$u_k(z,\omega) = \sum_{n=0}^{\infty} S(\omega)R^n(\omega)\{e^{i\upsilon(2nH+z)}e^{-\gamma|\upsilon|(2nH+z)} + e^{i\upsilon(2(n+1)H-z)}e^{-\gamma|\upsilon|(2(n+1)H-z)}\}, \qquad (3.2)$$

Where, $S(\omega)$ is the Fourier transform of the input waveform, $R(\omega)$ is the reflection coefficient, n is the reflected times by the base of the building, r is the damping ratio, v is the wave number. Submitting the equation (3.2) to the equation (3.1), the waveforms after deconvolution with the waveform on the top of the building can be expressed in the frequency domain as the equation (3.3).

$$D_{k,H}(z,\omega) = [e^{i\upsilon(z-H)}e^{-\gamma|\upsilon|(z-H)} + e^{i\upsilon(H-z)}e^{-\gamma|\upsilon|(H-z)}]/2 \qquad (3.3)$$

Based on equation (3.3), the waveform after deconvolved with the waveform of the top of the building (deconvolved wave) can be seen as the summation of one attenuating up-going wave (the first term) and one attenuating down-going wave (the second term). Based on the time difference between the down-going wave and the up-going wave of the deconvolved wave of the first floor (t_1) and the height of the building (H), average S-wave velocity traveling from the base to the top ($\bar{c}$) can be calculated from equation (3.4).

$$\bar{c} = 2H / t_1, \qquad (3.4)$$

Furthermore, based on the time differences between the down-going wave and up-going wave of the deconvolved waves of the k floor (t_k) and the k+1 floor (t_{k+1}), and the equivalent height between the k and the k+1 floor ($h_{k\to k+1}$), the shear-wave velocity traveling between the k floor and the $k+1$ floor can be known based on equation (3.5).

$$c_{k\to k+1} = 2h_{k\to k+1} / (t_k - t_{k+1}) \qquad (3.5)$$

3.2 Feasibility of Applying Deconvolution Method to Microtremor Records

Using the Deconvolution method, Snieder and Şafak have extracted the shear-wave velocity traveling within the Millikan Library in Pasadena, California from earthquake records of the building measured during the Yorba Linda earthquake of 3 September 2002. In this section, the feasibility of applying the Deconvolution method to microtremor records is proved through comparing shear-wave travel time extracted from microtremor records with that extracted from earthquake records and theoretical results analyzed based on the multi-degree-of-freedom RS model of the AIT-No.2 building. The view (north facade) of the AIT-No.2 building is shown in the Photo 5. Earthquake and microtremor measured floors are shown in the Figure 3 with marks ▼ and ○, respectively. Earthquake measurement was performed on the 6F and 1F of this building during the period of 1998~2006 with sampling rate of 100 Hz. Microtremors of the top and all the inner floors of this building were recorded recently with sampling rate of 100 Hz, 200 Hz, and 500 Hz with the purpose to examine the effect of sampling rate to reading error of shear-wave travel time.

Photo 5. The AIT-No.2 building

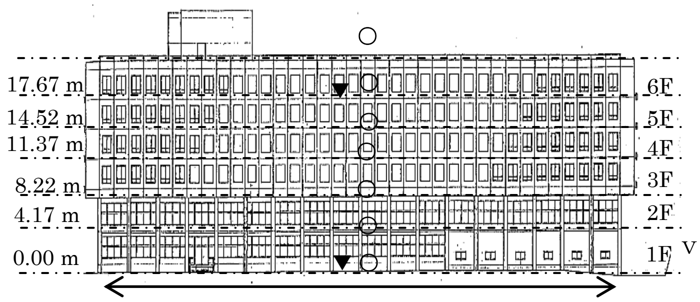

Figure 3. Earthquake measurement (▼)and microtremor measurement (○)

Because building responses to earthquakes depend on the amplitude, incidence azimuth, incidence angel, frequency characteristics of input motions, in this paper, twelve earthquake records with difference amplitude are selected. The relationships between the time difference t_1 (time difference between the down-going wave and up-going wave of the deconvolved wave of 1F) and the maximum velocities of the s-wave and coda-wave parts of the twelve earthquakes are shown in the Figure 4 with marks □ and ＊, respectively. From the Figure 4, it can be found that the time difference t_1 increases with the increasing of maximum velocities. If the maximum velocity increases more than 0.05 cm/s the t_1 becomes more than 0.14 sec. Deconvolved waves of the 1F which are calculated from the s-wave parts of maximum velocity more than and smaller than 0.05 cm/sec with the average of them are shown in the Figure 5 and the Figure 6, respectively. Those calculated using the coda-wave parts of all the twelve earthquakes are shown in the Figure 7. The t_1 extracted from the s-wave parts with maximum velocities> 0.05 cm/sec are 0.14 sec in both of the longitudinal and transvers direction. For the s-wave parts whose maximum velocities< 0.05 cm/sec, the t_1s are 0.12 sec in the longitudinal direction, and 0.10 sec in the transvers direction which are almost the same with those extracted from coda-wave parts considering the reading error of $1/f_{samp}$=0.01 sec.

Deconvolved waves calculated using the microtremor records with sampling rates of 100 Hz, 200 Hz, and 500 Hz are shown in the Figure 8. Based on the Figure 8, the time reading error of up-going waves and down-going wave becomes smaller with the increasing of sampling rate. Furthermore, because the time reading error of the microtremor records with f_{samp} of 100 Hz and 200 Hz are bigger than the travel time from the 6F to the top of the building, the time differences of the deconvolved waves of the 6F cannot be read. Comparing the t_1 extracted from microtremor records of f_{samp}=100 Hz with those extracted from coda-wave and s-wave parts with maximum velocity<0.05 cm/sec, we can find that they are almost the same.

Deconvolved waves calculated based on the multiple-degree-of-freedom RS model of the AIT-No.2 building (f_{samp}=200 Hz) are shown in the Figure 9. Comparing the Figure 9 with the Figure 8(c) and 8(d), we can find that the time difference between down-going waves and up-going waves of deconvolved waves extracted form microtremor records and the model are almost the same.

Comparing t_1 extracted from microtremor records with those extracted from earthquake records and with the theoretical results analyzed based on the model, we can find that they are almost the same Therefore, we conclude that it is feasible to extract shear-wave traveling time from microtremor records using the Deconvolution method. Furthermore, in order to read the time difference with higher precision, microtremor with higher sampling rate is necessary.

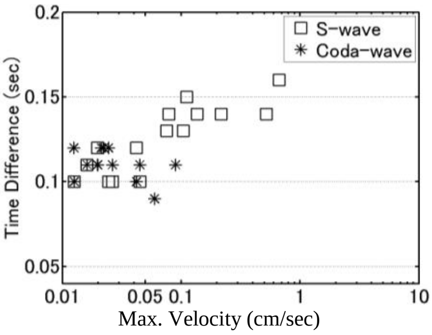

(a) Longitudinal

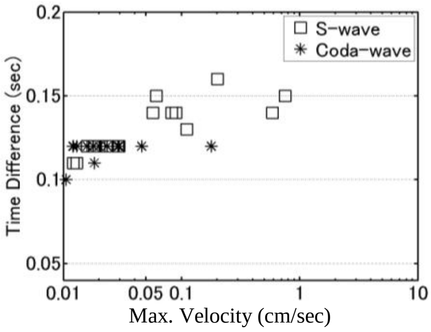

(b) Transvers

Figure 4. Relationships between the time difference t_1 and maximum velocity of s-wave parts (□) and coda-wave parts (*)

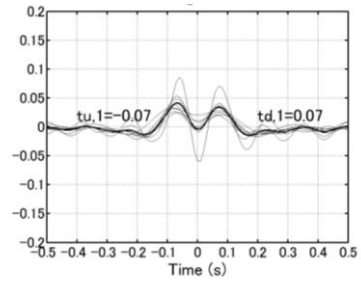

(a) Longitudinal

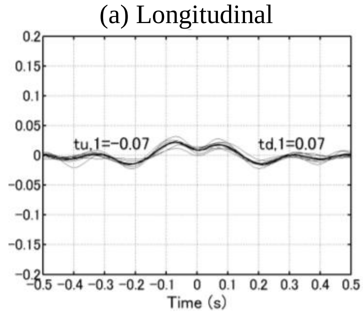

(b) Transvers

Figure 5. Deconvolved waves calculated using the s-wave parts with maximum velocity>0.05 cm/sec

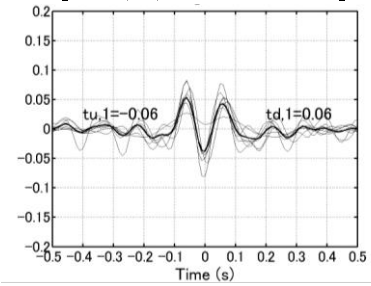

(a) Longitudinal

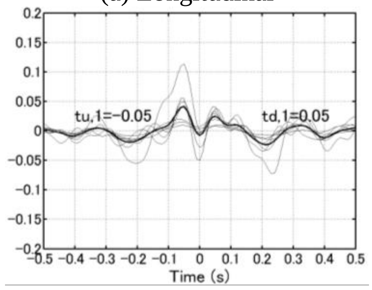

(b) Transvers

Figure 6. Deconvolved waves calculated using the s-wave parts with maximum velocity<0.05 cm/sec

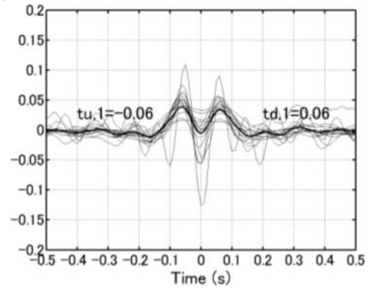

(a) Longitudinal

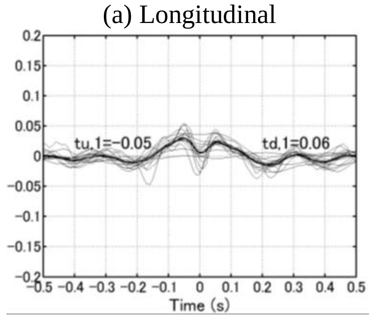

(b) Transvers

Figure 7. Deconvolved waves calculated using the coda-wave parts

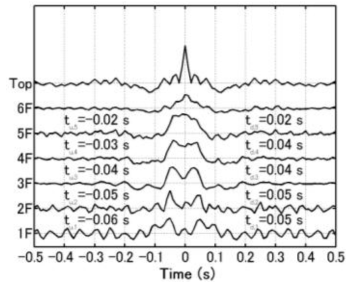

(a) Longitudinal

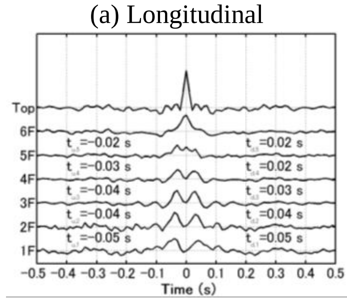

(b) Transvers

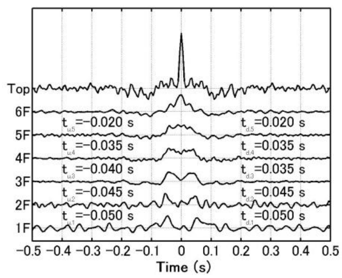

(c) Longitudinal

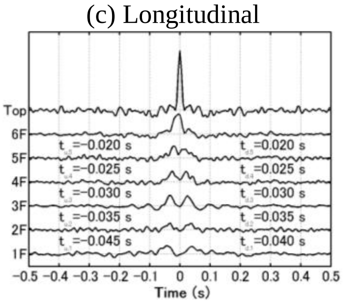

(d) Transvers

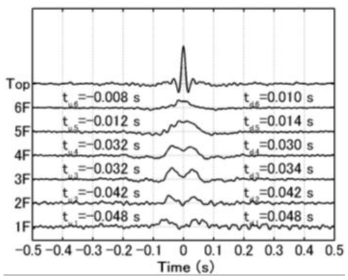

(e) Longitudinal

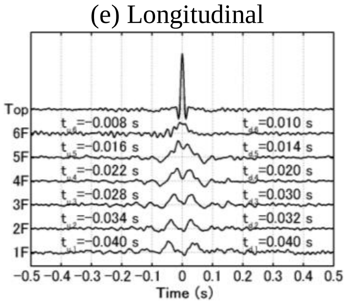

(f) Transvers

Figure 8. Deconvolved waves calculated using microtremor records; (a) and (b) correspond to sampling rate of 100 Hz; (c) and (d) correspond to sampling rate of 200 Hz; (e) and (f) correspond to sampling rate of 500 Hz

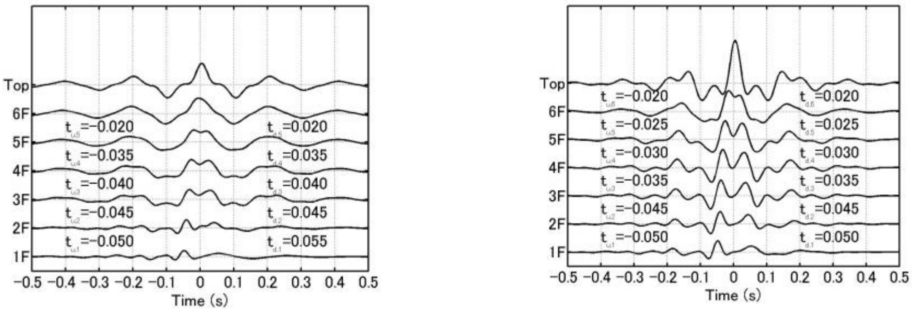

(a) Longitudinal (b) Transvers

Figure 9. Deconvolved waves calculated based on the MDOF model of the AIT-No.2 building

3.3. Shear-Wave Velocities of Building A~D

Deconvolved waves extracted from microtremor records measured on the Building A~D with sampling rate of 200 Hz are shown in the Figure 10. Using the corresponding time of down-going and up-going waves of deconvolved waves shown in the Figure 10, the distribution of shear-wave velocities of the Building A~C are calculated based on the equation (3.5) and the velocity distributions are shown in the Figure 11. Standard deviations are shown with thinner lines in this figure.

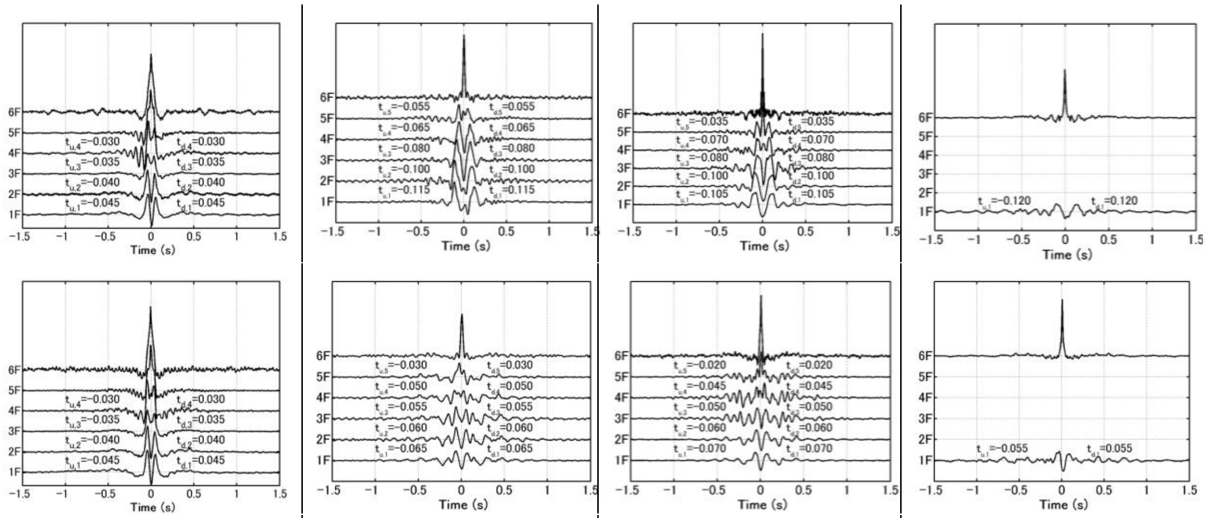

Building A | Building B | Building C | Building D

Figure 10. Deconvolved waves of the Building A~D; upper figures are results in the longitudinal directions, and lower figures are results in the transvers directions

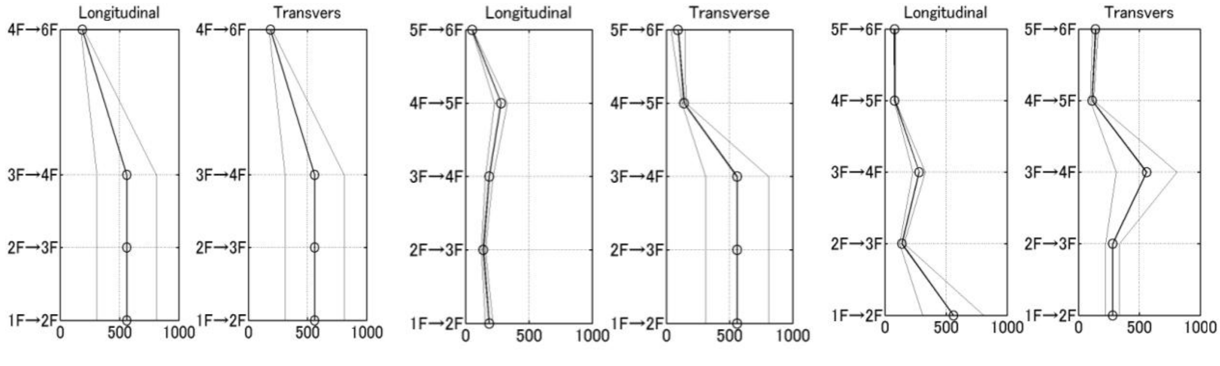

(a) Building A (b) Building B (c) Building C

Figure 11. Shear-wave velocity traveling between the k floor and the k+1 floor (kF→(k+1)F) of the (a)Building A, (b)Building B, and (c)Building C

Because the time difference of the 5th floor of the Building A cannot be read from the deconvolved wave, the shear-wave velocity traveling between the 4th floor to the 5th floor cannot be calculated. Therefore, in the Figure 11(a) shear-velocity traveling between the 4th floor to the 6th floor are shown instead. From Figure 11(a), we can find that the shear-wave velocities in the longitudinal direction and the transvers direction of the Building A are almost the same. Based on the Figure 11(b), we can find that shear-wave velocities in the longitudinal direction of the Building B are reduced to less than 300 m/sec, which are much slower than those in the transvers direction in the lower three stories of this building, which are almost the same with those extracted from the Building A. From the Figure 11(c), generally it can be found that the shear-wave velocities in both of the longitudinal and transvers direction of the Building C have dropped to almost less than 300 m/sec.

4. RESPONS FREQUENCIES

4.1 Building System Frequency f_{SYS}

Building system frequency f_{SYS} of the first mode are determined based on the predominant frequency of the power spectrum density of microtremor records of the 6F. Power spectrum density of the Building A~D are shown in the Figure 12.

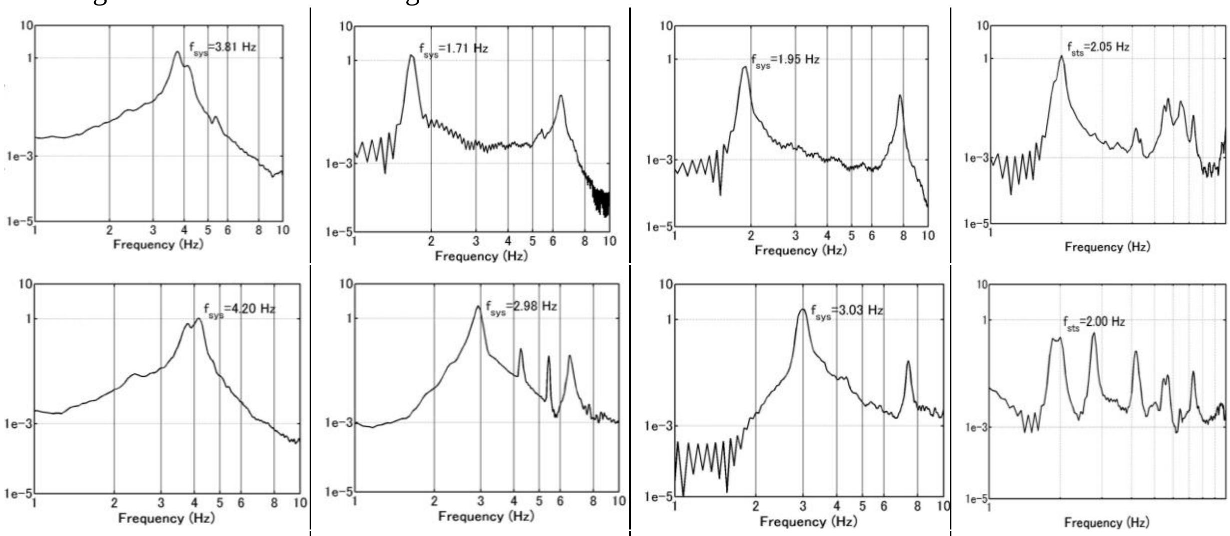

Building A | Building B | Building C | Building D

Figure 12. Power spectrum density of the Building A~D; upper figures are results in the longitudinal directions, and lower figures are results in the transvers directions

4.2 Response Frequency of Upper Structure f_B

The time difference t_1, average shear-wave velocities traveling from the base to the top ($\bar{c}$), and the response frequencies f_B of the upper structures of the Building A~D are shown in the Table 4.1. Form Table 4.1 we can find that average shear-wave velocity $\bar{c}$ of those severely damaged Building B~D in the longitudinal directions are slower than those in the transvers directions. Comparing $\bar{c}s$ of severely damaged buildings with those of the Building A, we can find that $\bar{c}$ $\bar{c}s$ of severely damaged buildings in the longitudinal direction reduced to less than 200 m/sec which is almost the half of that of the Building A. the response frequency f_B of those severely damaged buildings are reduced to less than the half of that of the Building A in the longitudinal directions.

Table 4.1. Time difference t_1, average shear-wave velocity $\bar{c}$, and response frequency f_B

Building	A		B		C		D	
	L*	T**	L	T	L	T	L	T
t_1 (sec)	0.090	0.090	0.230	0.130	0.210	0.140	0.240	0.110
$\bar{c}$ (m/sec)	373	373	146	285	160	240	140	305
f_B (Hz)	5.56	5.56	2.17	3.85	2.38	3.57	2.08	4.55

*L: longitudinal direction; **T: transvers direction

4.3 Apparent Frequency f_{APP}

Transfer functions of microtremor records of the Building A~D are shown in the Figure 13. The apparent frequency f_{APP} are determined based on the predominant frequency of transfer functions.

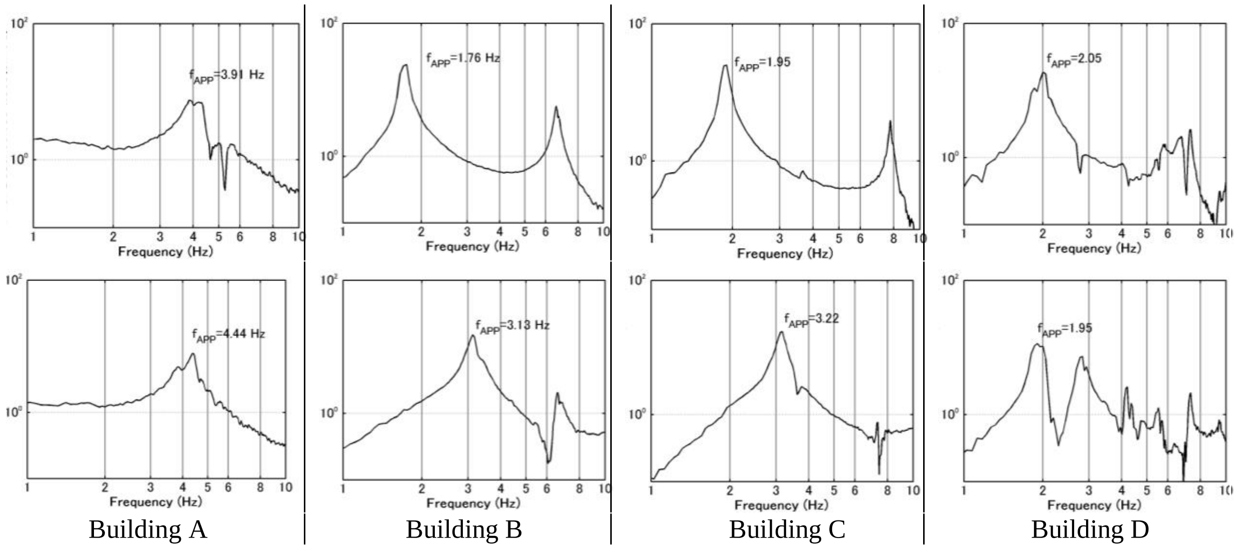

Figure 13. Transfer function of the Building A~D; upper figures are results in the longitudinal directions, and lower figures are results in the transvers directions

4.4 Rigid-Body Rocking Frequency f_R and Sway Frequency f_S

Rigid-body rocking frequency f_R can be estimated based on the approximate relationship between f_{APP}, f_B, and f_R as shown in equation (4.1). Using the response frequencies f_B solved in the section 4.2 and f_{APP} solved in the section 4.3, the rigid-body rocking frequency f_R can be solved based on the equation (4.1)

$$\frac{1}{f_{APP}^2} \approx \frac{1}{f_B^2} + \frac{1}{f_R^2} \tag{4.1}$$

Based on the approximate relationship between f_{SYS}, f_{APP}, and f_S as shown in equation (4.2), the rigid-body sway frequency f_S can be calculated.

$$\frac{1}{f_{SYS}^2} \approx \frac{1}{f_{APP}^2} + \frac{1}{f_S^2} \tag{4.2}$$

Using the response frequencies f_{SYS} solved in the section 4.1 and f_{APP} solved in the section 4.3, rigid-body sway frequency f_S can be solved based on the equation (4.2). Results of all the response frequencies are shown in the Table 4.2.

Table 4.2. Response frequencies of the Building A, B, C, and D

Building	f_{SYS} (Hz)		f_B (Hz)		f_{APP} (Hz)		f_R (Hz)		f_S (Hz)	
	L	T	L	T	L	T	L	T	L	T
A	3.81	4.20	5.56	5.56	3.91	4.44	5.49	7.39	17.14	10.99
B	1.71	2.98	2.17	3.85	1.76	3.13	2.99	5.36	7.30	9.84
C	1.95	3.03	2.38	3.57	1.95	3.22	3.42	7.48	∞ *	8.83
D	2.05	2.00	2.08	4.55	2.05	2.88	11.60	3.72	∞	2.78

* ∞ : means infinite.

5. CONCLUSIONS

In this paper, quantitative damage criteria of severely damaged 6-story masonry buildings are studied based on the combination of time-domain and frequency-domain analysis of building response parameters. The following conclusions are obtained.

1. The feasibility of applying deconvolution with the waveforms of the top of the building (Deconvolved method for short) to microtremor records to extract the time-domain building

response parameters, i.e. the shear-wave velocity traveling in the upper structures, are proved based on the comparison between shear-wave travel times extracted from microtremor records and those extracted from earthquake records and with the theoretical results calculated based on multiple-degree-of- freedom RS model of the measured building.

2. Shear-wave velocities traveling within inner stories of the Building A which is the sound one are almost the same in the longitudinal and transvers directions with the value of about 560±200 m/sec in the lower three stories. For the severely damaged Building B, shear-wave velocities in the transvers direction are almost the same with those of the Building A, while in the transvers direction they are reduced less than 300 m/sec. We conclude that the damage of the Building B is more serious in the longitudinal direction than in the transvers direction. In the Building C, which is also a severely damaged one, shear-wave velocities traveling within inner stories reduced to less than 300 m/sec happened in both of the two directions, especially in the second story which corresponding to the visual damage of this story.
3. Response frequency of the upper structure (f_B) determined based on the shear-wave travel time from the base to the top of buildings only depends on the properties of upper structures. The f_Bs of the Building A in the longitudinal and transvers direction are the same with the value of 5.56 Hz. For damaged buildings B~D, f_Bs reduced to less than 2.5 Hz which is almost the half of that of the Building A in longitudinal directions.
4. Comparing f_Bs and apparent frequencies f_{APP}s, we can find that f_Bs are much higher than f_{APP}s. This should be attributed to the nonnegligible effect of the rigid-body rocking. Therefore, in order to estimate structure damage correctly, the f_B which is independent on the ground coupling are more feasible than the f_{APP}.
5. Base on the comparison between f_R in the longitudinal direction and that in in the transvers direction, we can find that the f_R in the longitudinal direction is bigger than that in the transvers direction for the Building A~C, while for the Building D it is revers. This should be attributed to the different orientation of the Building D (longitudinal direction is N-S) from the Building A~C.
6. Because the f_{APP} and the f_{SYS} of Building C and D are the same, the f_S calculated based on these two terms becomes to infinite. Based on the comparison between f_R and f_S of each building, we find out that the f_R are smaller than f_S for Building A~C.

REFERENCES

Zhang, M. Z. and Y. J. Jin (2008) "Building damage in Dujiangyan during M8.0 Wenchuan earthquake," **J. Earthquake Engineering and Engineering Vibration 7(3)**, 263-269.(in Chinese)

Luco, J. E., Trifunac, M. D. and Wong, H. L.(1987): On the apparent change in the dynamic behavior of a nine-story reinforced concrete building, **Bull. Seismol. Soc. Am. 77, no.6,** pp. 1961-1983.

Todorovska, M. I. (2009): Seismic Interferometry of a soil-structure interaction model with coupled horizontal and rocking response, **Bull. Seismol. Soc. Am. 99, no. 2A**, pp. 611-625.

Ohba, S. and T. Fukuda (1999) "Changes in natural frequency of apartment buildings before and after the Hyogoken-nanbu earthquake -Part 1. microtremor measurements of apartment buildings," **Summaries of Technical Papers of Annual Meeting** Sep.,1999, pp. 345-346.

Tsurumura, K. and H. Kawase (2008) "Comparison of dynamic properties of low and mid-rise RC buildings before and after the earthquake based on microtremor measurement," ***J. Struct. Constr. Eng.*, AIJ, Vol. 73 No. 627**, 717-723, May.

Sato, T. Y. Nakamura and Saita, J. (2008) "The change of the dynamic characteristics using microtremor," **The 14th World Conference on Earthquake Engineering**, October 12-27, 2008, Beijing, China.